Correia, M. J., Schwarzacher, W., Chagas, E. F., & Figueiredo, W. (2016). Magnetic relaxation of nanoparticles with cubic and uniaxial anisotropies. Journal of Physics: Conference Series, 686(1), [012009]. DOI: 10.1088/1742-6596/686/1/012009

Magnetic relaxation of nanoparticles with cubic and uniaxial anisotropies

2016 J. Phys.: Conf. Ser. 686 012009

(http://iopscience.iop.org/1742-6596/686/1/012009)

Journal of Physics: Conference Series **686** (2016) 012009 doi:10.1088/1742-6596/686/1/012009

Magnetic relaxation of nanoparticles with cubic and uniaxial anisotropies

Marcos J. Correia[1,2], Walther Schwarzacher[2], Edson Ferreira Chagas[2,3] and Wagner Figueiredo[1]

[1]Departamento de Física, Universidade Federal de Santa Catarina,88040-970, Florianópolis, Brasil.
[2]H. H. Wills Physics Laboratory, University of Bristol, BS8 1TL, Bristol, UK.
[3] Instituto de Física, Universidade Federal de Mato Grosso, 78060-900 - Cuiabá, MT,Brasil.

E-mail: wagner.figueiredo@ufsc.br

Abstract. We use Monte Carlo methods to simulate the influence of Brownian rotation on the magnetic properties of a system of single-domain magnetic nanoparticles with cubic and uniaxial magnetic anisotropies. The distinguishing feature of the system is a strongly temperature-dependent viscosity. Such a system has been realized experimentally using magnetic nanoparticles suspended in a freeze-concentrated cryoprotectant solution.

In this work we investigate magnetic phenomena related to the rotation of magnetic nanoparticles, by employing the Brown relaxation theory [1], during the transition between frozen and unfrozen states of the system. We developed a computational method to calculate the magnetic properties related to this process. We consider a system composed of single-domain magnetic nanoparticles dissolved in a solvent that also contains a cryoprotectant. On freezing the solvent, a thin liquid layer consisting of solvent and freeze-concentrated cryoprotectant forms around each nanoparticle. The glass transition temperature of this liquid layer T_g is lower than the freezing temperature of the solvent. In this way, while the solvent is already frozen, the freeze-concentrated cryoprotectant still permits nanoparticles to rotate. Initially, the system is found in a temperature below T_g, that is, without any rotational freedom. Increasing the temperature, the system passes through T_g, so that the nanoparticles become completely free to rotate. This behavior was observed experimentally in Reference [2], where magnetic measurements were used to monitor the behavior of single-domain magnetite nanoparticles doped with 2.5 % cobalt enclosed by the near-spherical cage protein ferritin (CMF) in a freeze-concentrated cryoprotectant solution.

In order to study this system through simulations we employed the Monte Carlo method along with the Metropolis algorithm. We calculate the energy of a new configuration of the system just after a small variation in the direction of the magnetic moment of a nanoparticle randomly chosen. Then, we compare this energy with the previous one to accept or not the new configuration of the system [3, 4, 5]. Besides this procedure we also included the change in energy due to the rotation of the nanoparticle in the viscous medium.

We consider a set of N non-interacting single-domain magnetic nanoparticles. We adopt the following effective energy model [3, 6, 7]

$$E_a = -\sum_{i=1}^{N} K_{ui}\,(\vec{S_i}.\vec{e_{1i}})^2 - \frac{1}{2}\sum_{i=1}^{N}\sum_{j=1}^{3} K_{ci}\,(\vec{S_i}.\vec{e_{ji}})^4 - \sum_{i=1}^{N} \vec{H}.\vec{\mu_i}, \tag{1}$$

where $K_{ui} = k_u V_i$, and $K_{ci} = k_c V_i$ are the uniaxial and cubic anisotropies of a particle of volume V_i, respectively. In this study the anisotropy density constants k_u and k_c are assumed to be both positive, and we also define the relative anisotropy parameter $k_{uc} = k_c/k_u$. The volume V_i of the i^{th} particle is selected from a log-normal distribution. The magnetic moment of the i^{th} particle is written as $\vec{\mu_i} = \mu_i \vec{S_i}$, where $\vec{S_i}$ is a unit vector, $\mid \vec{S_i} \mid = 1$, and $\mu_i = m_s V_i$, with m_s the particle magnetization. In the above equation the vectors $\vec{e_{ji}}$ $(j = 1, 2, 3)$ are unit vectors parallel to the cubic axes of the i^{th} particle.

In the case of rotational Brownian motion we consider also the energy contribution E_r

$$\frac{dE_r}{dt} = \sum_{i=1}^{N} 2\pi r_i^3 \eta \omega_i^2, \tag{2}$$

where η is the viscosity, r is the hydrodynamic radius and ω is the angular velocity. For a liquid whose temperature is close to the glass transition T_g, the viscosity η can be described by the empiric equation of Vogel-Fulcher-Tammann (VFT) [8, 9, 10]

$$\eta = \eta_0 \exp\left[\frac{DT_0}{T - T_0}\right], \tag{3}$$

where T_0 corresponds to a temperature for which η is very high, η_0 is a reference viscosity, and D is a constant which depends on the structure of the system [11]. Therefore, in our calculations we need to take into account the total energy $E = E_a + E_r$, that is, the magnetic and rotational energy contributions.

Besides making a change in the direction of the magnetic moment of the nanoparticle, we also make a change in the direction of its magnetic easy axis. This is necessary in order to take into account the physical rotation of the nanoparticle in the viscous medium. After we change both directions, magnetic moment and easy axis, we compute the variation in the total energy ΔE. When $\Delta E < 0$, both changes are accepted. On the other hand, if $\Delta E > 0$, we generate a random number A, uniformly distributed between zero and one. If $A < \exp(-\Delta E/k_B T)$, the new configuration is accepted, if not, we keep the original configuration.

We consider a competition between the cubic and uniaxial anisotropies [15, 12, 13] as in the corresponding experimental CMF system. The size of the particles are selected from a log-normal distribution with mean value $V_0 = 1$ and standard deviation $\sigma = 0.25$, in agremeent with the experimental data [2, 12].

In Fig. 1 we give the values of the reduced magnetization, which is defined by $m = \mu H/K_0$, as a function of the reduced temperature $t = k_B T/K_0$, where $K_0 = k_u V_0$ and the viscosity is $\eta = 10^{-12} \exp[3/(t - 0.33)]$. The open squares represent the non-aligned system (cooled to $t = 0$ at zero field), while the full squares represent the aligned system (cooled at t = 0, but in a strong magnetic field, $h = 20$). For the aligned system we do not observe a blocking temperature, and this is due to the fact that all the magnetic moments were already aligned in the direction of the applied field. Increasing the temperature, we observe a decrease in the magnetization. For the non-aligned case, we see that the magnetization increases with the temperature up to the blocking temperature. When $t \geq t_b = 0.14$, both systems, aligned and non-aligned, show a decrease in the magnetization as a function of temperature. However,

the magnetization of the aligned system is always higher than the non-aligned one up to the temperature $t = 0.45$. Close to $t = 0.45$, the magnetization of the aligned system drops abruptally, assuming the same value as the non-aligned one. At this temperature, which we denote by T_R, and which is three times larger than t_b, the value of the viscous energy E_r is close to the magnetic energy associated with the magnetic anisotropy allowing nanoparticles to rotate due to the rotational brownian motion. From this temperature on, both systems become magnetically equivalent, where all the easy magnetization axes point randomly in space.

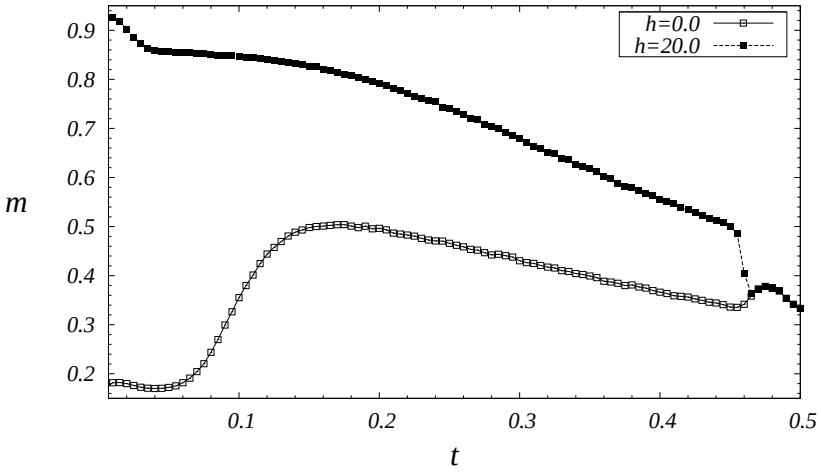

Figure 1. Reduced magnetization m as a function of temperature for a system with $\sigma = 0.25$, $k_{uc} = 2$, viscosity η. A small magnetic field $h = 0.5$ is applied during the heating process. The open squares represent the system initially cooled to $t \approx 0$ at zero field and the full squares represent the system initially cooled to $t \approx 0$ in an external field $h = 20$. The error bars are smaller than the size of the symbols, and the lines serve as a guide to the eyes.

Figure 2 shows the reduced magnetization m as a function of the external magnetic field h for two similar systems, but different cooling processes. In the first case, represented by the cross symbols, the system was cooled below T_0 ($t = 0.33$) in the presence of a strong magnetic field $h = 20$, from $t = 0.55$ to $t = 0.01$. In the second case the system was cooled below T_0 in a zero magnetic field, which is represented by the squares. We note a clear difference between the two hysteresis curves. The system cooled in a strong field keeps the easy magnetization axes partially aligned to the field, which results in larger coercive fields when compared to the system cooled in the absence of a field, in which the directions of the easy axes are completely randomly distributed.

The applied field during the cooling process causes the rotation of the nanoparticle, and this is the reason that we observe the alignment of the magnetization easy axes. The alignment is not complete because T_R is roughly three times larger than the blocking temperature of the system, as can be seen in Fig. 1. However, the alignment is sufficient to change the magnetic properties of the system. This feature is in agreement with the experimental result [2].

In Fig. 3, we show magnetization curves, when the system is cooled from high temperature, $t = 0.52 > T_R$ to $t = 0.42 < T_R$, in the presence of an external magnetic field h, then to t=0 in zero field. The field is turned off at $t = 0.42$, which is larger than t_b, so the magnetic moments can cross the energy barriers, and the system can relax to very small values of the magnetization. However, as the system is already immobile, their magnetization easy axes can not rotate leaving the system with a partial alignment dependent on the applied field h. We note in Fig. 3 that the blocking temperature does not depend on the system alignment, however,

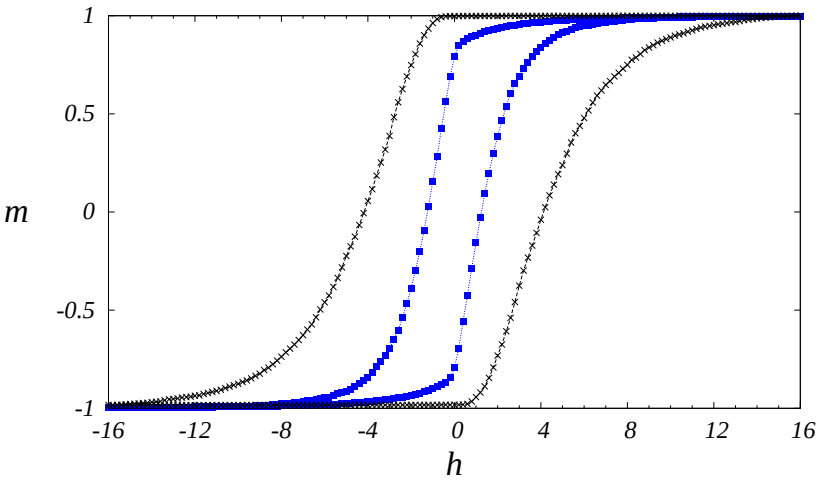

Figure 2. Hysteresis curves for the temperature $t = 0.02$ and $k_{uc} = 2$. The cross symbols, represent the system aligned by an external magnetic field, while the squares represent the system cooled in the absence of a field. The error bars are smaller than the size of the symbols, and the lines serve as a guide to the eyes.

the maximum value of the magnetization depends on the applied field during the cooling process, and after we reach the temperature T_R, all the curves have the same behavior as a function of temperature.

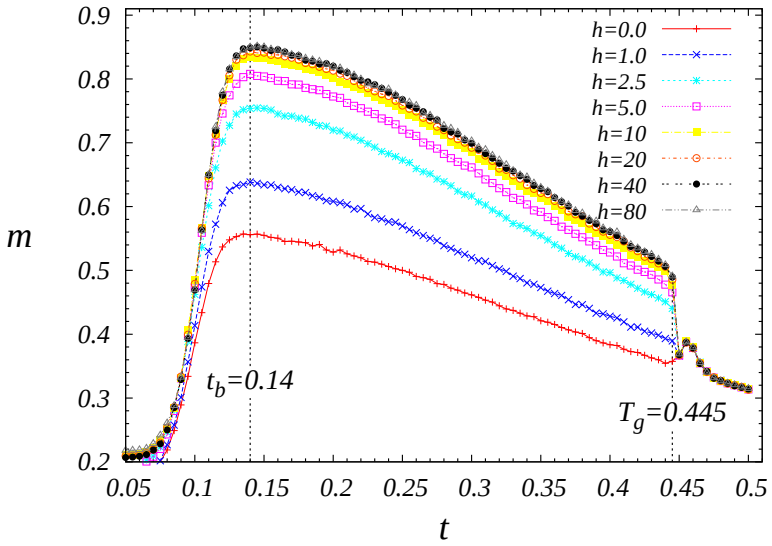

Figure 3. Magnetization curves for a system cooled in different values of the magnetic field (see text). We use the following set of parameters: $\sigma = 0.25$, $k_{uc} = 2$ and viscosity η. During the heating process we apply a small magnetic field $h = 0.5$. The error bars are smaller than the size of the symbols, and the lines serve as a guide to the eyes.

Figure 4 shows experimental magnetization curves for different values of the field applied during the cooling process. The system is similar to the one presented in Reference [2]. Qualitatively, the simulations shown in Fig. 3 and the experimental results agree very well.

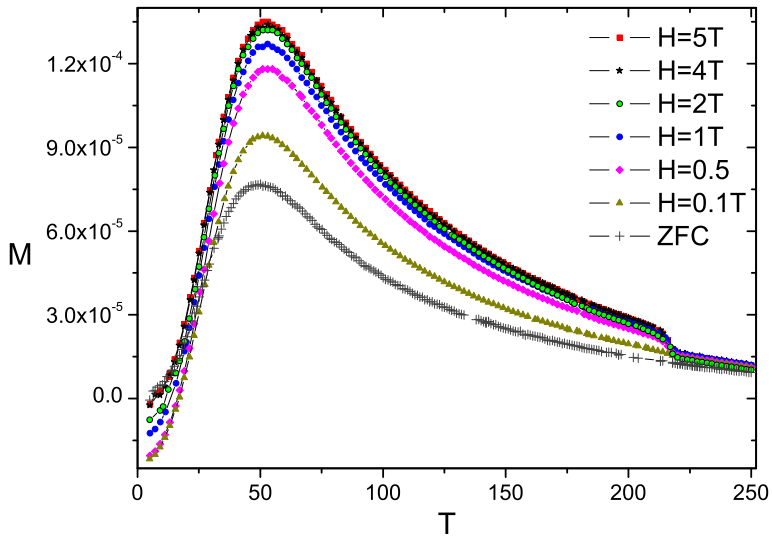

Figure 4. Experimental magnetization data for CMF cooled in the presence of different magnetic fields. Each system was cooled from temperature $250K$ to $200K$. During the heating process a small magnetic field $H = 0.05T$ was applied. Magnetic moments M are given in emu units, and temperature in K. The error bars are smaller than the size of the symbols.

The reduced magnetization as a function of the computational time (t_c), measured in Monte Carlo steps (MCs), for different temperatures, is shown in Fig. 5. In this case we have discarded the first 400 MCs, because in this time interval the Néel relaxation is dominant. The dashed black line is the fitting performed on the relaxation curves using the equation

$$y = M_0 \exp(-t_c/\tau_B), \tag{4}$$

where M_0 is a quantity related to the magnetization of the system after 400 MCs and τ_B is the Brown relaxation time. We consider the following temperatures: $t = 0.456$, $t = 0.458$, $t = 0.460$, $t = 0.462$, $t = 0.464$, and $t = 0.466$. From the fitting of these curves using eq. 4, we obtain the values of τ_B as a function of the temperature.

The behavior of the quantity $|\cos(\theta)|$, where θ is the mean angle made by the easy axis with the direction of the applied field, as a function of the number of Monte Carlo steps is shown in Fig. 6. At high temperatures and after a long time, the value of $|\cos(\theta)|$ reaches a minimum of around 0.55. This value is close to that expected for a completely random system, where $|\cos(\theta)| = 0.50$. In the figure the dashed line is the fitting employing the eq. $y = C_0 \exp(-t_c/\tau_B)$, where C_0 is related to the initial value of $|\cos(\theta)|$. We also found values of τ_B from the relaxation of $|\cos^2(\theta)|$, and the values of τ_B determined from this quantity, $|\cos(\theta)|$ and m are compared in Figure 7. In previous experimental studies [2] m was assumed to be proportional to $|\cos^2(\theta)|$ but from Fig. 7, though the values of τ_B determined from all the different quantities are similar, the values determined from m are closer to those determined from $|\cos(\theta)|$ than those determined from $|\cos^2(\theta)|$.

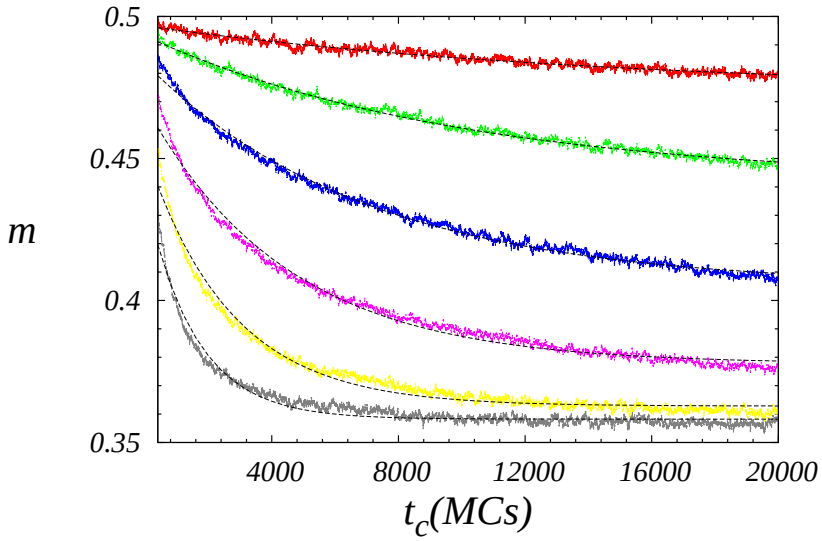

Figure 5. Reduced magnetization m as a function of the computational time measured in Monte Carlo steps in the presence of a small field $h = 0.5$. The parameters of the system are $\sigma = 0.25$, $k_{uc} = 2$. The system was cooled in the presence of a field $h = 20$. The temperatures are: $t = 0.456$, red curve, $t = 0.458$, green curve, $t = 0.460$, blue curve, $t = 0.462$, pink curve, $t = 0.464$, yellow curve and $t = 0.466$, grey curve. The dashed lines are fits using Eq. 4.

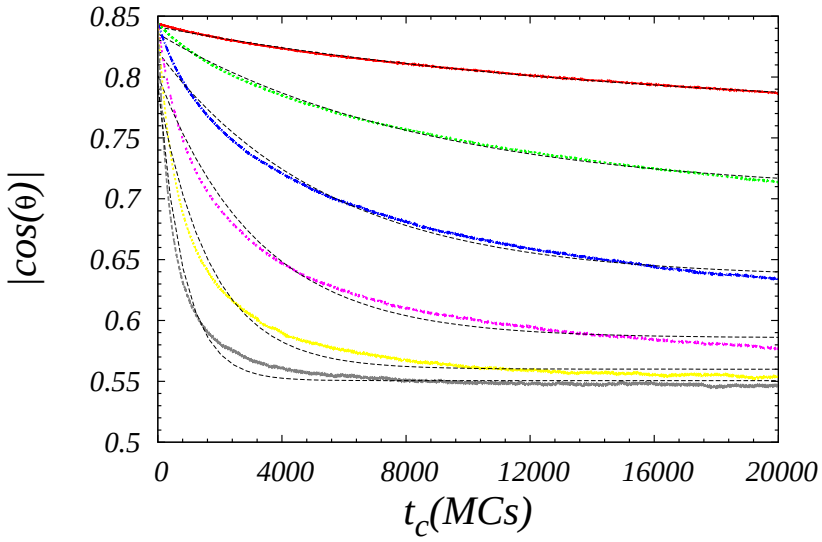

Figure 6. $|\cos(\theta)|$ (see text) as a function of the computational time measured in Monte Carlo steps in the presence of a small magnetic field $h = 0.5$, $\sigma = 0.25$, and $k_{uc} = 2$. The system was cooled in the presence of a field $h = 20$. Curves, red $t = 0.456$, green $t = 0.458$, blue $t = 0.460$, pink $t = 0.462$, yellow $t = 0.464$, and grey $t = 0.466$.

ACKNOWLEDGMENTS

M. J. Correia, Edson F. Chagas and W. Figueiredo would like to acknowledge the Brazilian agency CNPq for the financial support. This work was also partially supported by INCT-

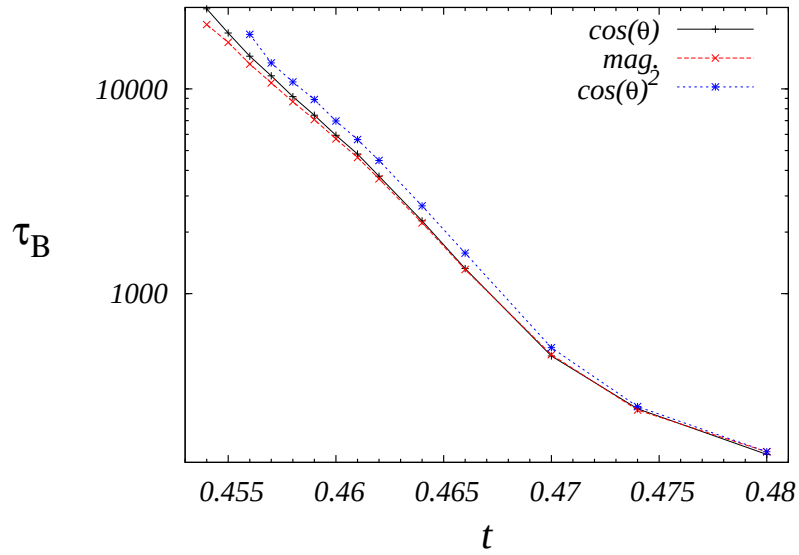

Figure 7. Determination of τ_B as a function of the reduced temperature, using three different procedures, as indicated in the figure.

FCX (FAPESP-CNPq). W. Schwarzacher would like to thank the Engineering and Physical Sciences research Council and the European Community's Seventh Framework Programme (FP7/2007–13) under Grant Agreement no. 228673(MAGNONICS).

References

[1] Brown W F 1959 *J. Appl. Phys.* **30** 130S
[2] Eloi J C, Okuda M, Jones S E and Schwarzacher W 2013 *Biophysical Journal* **104** 2681
[3] Figueiredo W and Schwarzacher W 2008 *Phys. Rev. B* **77** 104419
[4] Landau D P and Binder K 2009 *A Guide to Monte Carlo Simulations in Statistical Physics* (Cambridge University Press,Cambridge)
[5] Nowak U, Chantrell R W and Kennedy E C 2000 *Phys. Rev. Lett.* **84** 163
[6] Garanin D A and Kachkachi H 2003 *Phys. Rev. Lett.* **90** 065504
[7] Djárdin P M, Kachkachi H, and Kalmykov Yu P 2008 *J. Phys. D: Appl. Phys.* **41** 134004
[8] Vogel H J 1921 *Physik Z* **22** 645
[9] Fulcher G S 1925 *J. Am. Ceram. Soc.* **8** 339
[10] Tammann G and Hesse W Z 1926 *Anorg. Allg. Chem.* **156** 245
[11] Dagdug L 2000 *J. of Phys. Cond. Matt.* **12** 9573
[12] Okuda M, Eloi J -C, Sarua A, Ward Jones S E, and Schwarzacher W 2012 *J. Appl. Phys.* **111** 07B519
[13] Eloi J -C, Okuda M, Carreira S, Schwarzacher W, Correia M J and Figueiredo W 2014 *J. Phys. Condens. Matter.* **26** 146006
[14] Néel L 1949 *Ann. Geophs. (C.N.R.S.)* **5** 99
[15] Correia M J, Figueiredo W and Schwarzacher W 2014 *Phys. Let. A* **378** 3366
[16] Hartmann U and Mende H H 1985 *Phil. M.* **52** 889-897